Nature Methods

Miniaturized integration of a fluorescence microscope

Kunal K Ghosh, Laurie D Burns, Eric D Cocker, Axel Nimmerjahn, Yaniv Ziv, Abbas El Gamal & Mark J Schnitzer

Supplementary Figure 1	An array of integrated microscopes can facilitate parallel imaging applications.
Supplementary Figure 2	The integrated microscope enables Ca^{2+} imaging studies of CA1 hippocampal pyramidal neurons in freely behaving mice.
Supplementary Table 1	CMOS image sensor specifications and characterization results.
Supplementary methods	

Note: Supplementary video 1 is available on the Nature Methods website.

Supplementary Figure 1 | An array of integrated microscopes can facilitate parallel imaging applications.

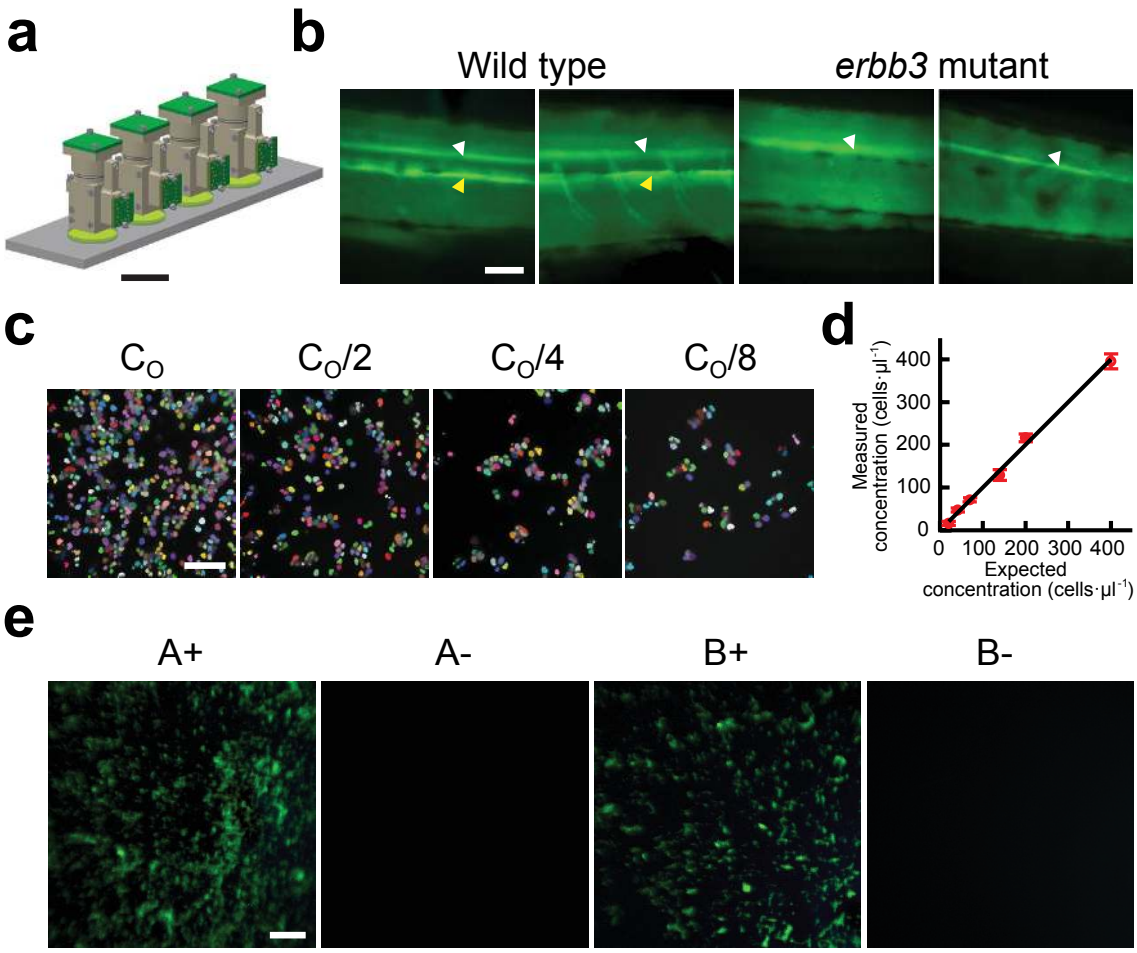

a. Schematic of four microscopes assembled in an array. Scale bar is 1 cm.

b. Multiple microscopes reveal phenotypes of wild-type and *erbb3* mutant zebrafish after fluorescence immunolabeling of myelin basic protein with Alexa-488. White arrowheads mark spinal cords. Yellow arrowheads mark the posterior lateral nerve in wildtype fish. In *erbb3* fish Schwann cells fail to develop on this nerve. Each image was taken by a different microscope and has undergone subtraction of background fluorescence. Scale bar of 50 µm applies to all panels, which show 225 × 225 pixel areas of the image sensor.

c. Integrated microscopes enable accurate cell counting assays in 96-well plates. A base concentration ($C_O \approx 4.0 \times 10^5$ cells/mL) of live MCF7 human breast cancer cells labeled with carboxyfluorescein was serially diluted, with eight sample wells for each of six concentrations. An automated algorithm counted the cells in the images (**Supplementary Note 1**). The panels show counting results, with individual cells identified at four different concentrations shown in color. Four different microscopes acquired the images. Scale bar of 100 μm applies to all images, which show 400 × 400 pixel regions of the image sensor.

d. Measured cell concentrations versus the expectation based on sample dilution. A linear fit (solid line) has $r^2 = 0.995$. Error bars represent s.e.m. from the $n = 8$ samples from each dilution.

e. Samples stained with auramine-O and imaged with the integrated microscope distinguish the two cultured specimens positive for TB (A^+ and B^+) from the two negative control specimens placed on the same slides (A^- and B^-). Scale bar of 50 μm applies to all images, which show 300 × 300 pixel regions of the image sensor.

Supplementary Figure 2 | The integrated microscope enables Ca^{2+} imaging studies of CA1 hippocampal pyramidal neurons in freely behaving mice.

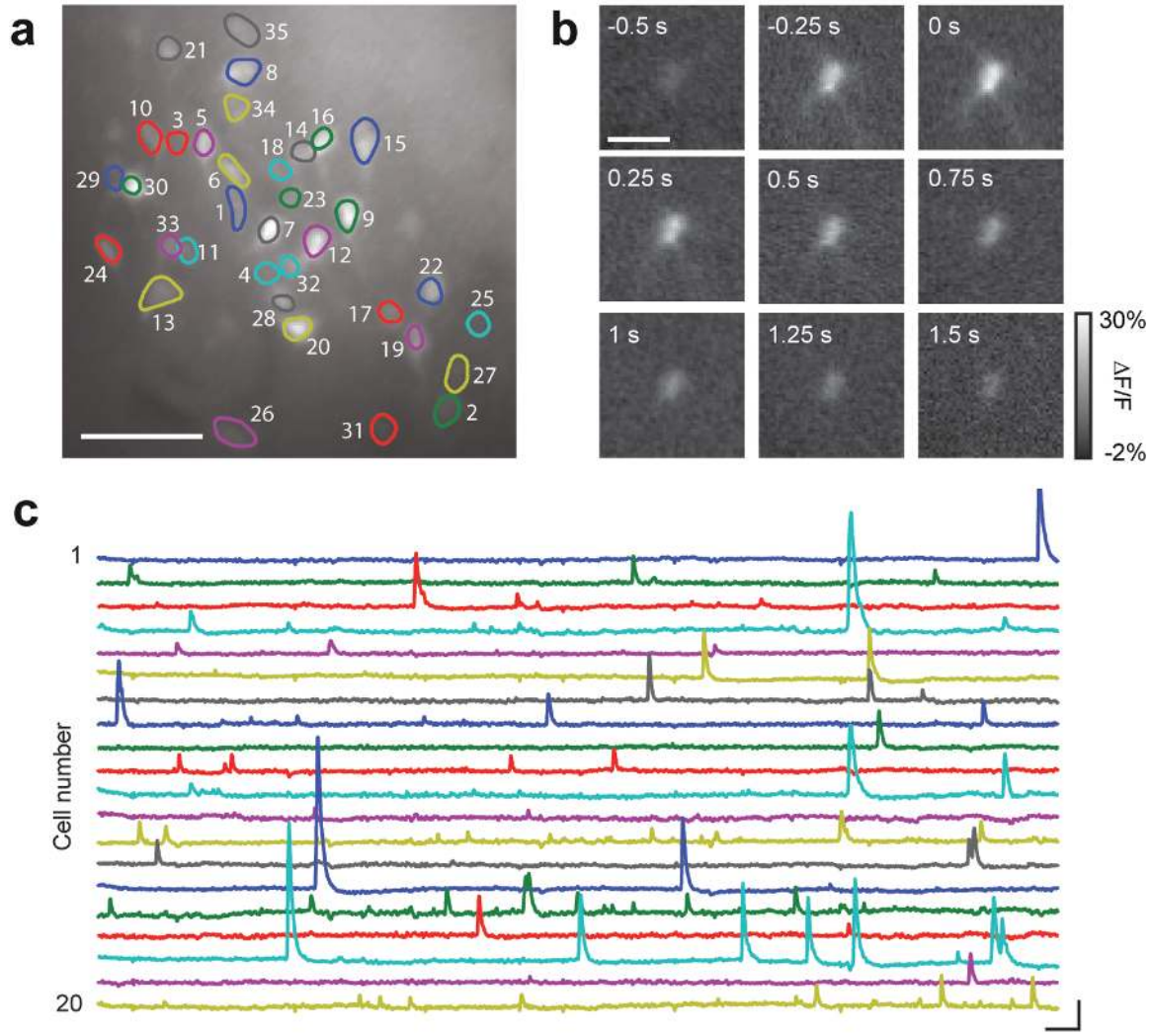

a. Contours of 36 CA1 pyramidal neurons identified by Ca^{2+} imaging in a freely behaving mouse, superimposed on a fluorescence image (320 × 320 pixel sub-region of the sensor; 200-600 μW illumination power at the specimen plane) of the CA1 area that is an average over the experiment's entire imaging duration (55 min). Pyramidal neurons expressed the GCaMP3 Ca^{2+}-indicator under the control of the CaMKIIα promoter. Scale bar is 100 μm.

b. Image sequence displaying relative changes in fluorescence ($\Delta F/F$) observed during a representative Ca^{2+} transient for cell 9 in (**a**). The timestamps provide the temporal interval relative to the time of the maximum $\Delta F/F$ increase. Scale bar is 50 μm. All panels show the same 100 × 100 pixel sub-region from (**a**).

c. Traces of relative fluorescence changes for 20 neurons identified in (**a**), acquired while the mouse explored a square, open field arena. Scale bars are 10 s (horizontal) and 5% $\Delta F/F$ (vertical).

Nature Methods:doi10.1038/nmeth.1694

Supplementary Table 1 | CMOS image sensor specifications and characterization

Maximum frame rate*	36 Hz (at 640 × 480 pixels)
Pixel read noise	10 electrons per pixel
Dark current (at room temp.)	0.15 fA
Dark signal non-uniformity	0.005 fA
Full well capacity	52,000 electrons per pixel
Peak signal-to-noise-ratio	47 dB
Dynamic range	60 dB
Quantum efficiency	0.6 (at 530 nm)
Digitization	10 bits

*Higher frame rates possible over smaller regions of interest (*e.g.* 100 Hz at 300 × 300 pixels)

Supplementary Methods

Imaging of zebrafish

Sample preparation

A batch of 50 zebrafish 5 days post-fertilization, comprising an unknown mix of wild type and Schwann cell-deficient *erbb3* mutants, were fixed and fluorescently immunostained for Myelin Basic Protein (MBP). In brief, we fixed zebrafish in 2% Paraformaldehyde powder (PFA) plus 1% Trichloroacetic acid (TCA) freshly dissolved in Phosphate buffered saline (PBS) for 10 min at room temperature with gentle rocking. We washed the zebrafish several times in PBS plus 0.8% Triton X-100 (PBT), followed by additional washes in distilled water, acetone, distilled water, and PBT, in that order. Zebrafish underwent blocking with PBT plus 10% normal goat serum (NGS, Jackson Immuno Laboratories 005-000-121) for 1 h at room temperature, followed by overnight incubation with the primary antibody (anti-MBP1) in PBT plus 2% NGS, at 4°C with gentle rocking. We then performed several PBT washes of 15-30 min and incubated the zebrafish for 3 hours at room temperature with goat secondary antibody conjugated to fluorescent Alexa 488 diluted 1:2000 (AlexaFluor 488 goat anti-rabbit IgG, Invitrogen, A-11008) in PBT plus 2% NGS. We again performed several PBT washes of 15-30 min and then stored the zebrafish in PBT for 1 day before mounting, to reduce background staining.

Assay setup and imaging methods

We transferred all zebrafish from PBT onto a microscope slide and arranged the fish in consistent orientations, spaced such that multiple samples could be imaged in parallel. We covered the samples with No. 00 cover slips sealed with 70% glycerol applied to the

sides. We positioned four microscopes in a holder over the fish such that each microscope had the central portion of a zebrafish body within its field-of-view. All microscope LEDs were set to deliver ~600 μW to the specimen. Independent focusing and imaging control for each microscope permitted individual adjustments to be made as needed. We acquired images in sets of four, and for each set of images we also acquired a corresponding background image without the sample in focus, to correct for any illumination non-uniformities or background fluorescence originating from the slide. Images of **Supplementary Fig. 1b** are a representative set following background subtraction.

Cell counting assays

Sample preparation

We cultured MCF7 human breast cancer cells to 90% confluency and harvested the cells by trypsinization. After harvesting and centrifugation, ~10^7 cells were suspended in 37°C PBS containing 10 μM Vybrant Carboxyfluorescein diacetate, succinimidyl ester (CFDA-SE) (Invitrogen, V12883) and incubated for 15 min at 37 °C. Intracellular esterases convert CFDA-SE into a fluorescent marker via cleavage of the succinimidyl ester group. We pelleted the cells again by centrifugation and re-suspended them in fresh, pre-warmed Roswell Park Memorial Institute (RPMI) 1640 medium (Invitrogen, A10491-01) with 10% fetal bovine serum and 1% Penicillin/Steptomycin. The cells were incubated for another 30 min at 37 °C, re-pelleted by centrifugation, and re-suspended in the same medium, vortexed, and diluted in medium to yield a stock solution of $4 \cdot 10^5$ cells/mL. We performed five further 1:2 serial dilutions in medium. We analyzed a sample of each dilution by flow cytometry (FACSCalibur, BD Biosciences, San Jose) to

determine the cell concentrations shown on the *x*-axis of **Supplementary Fig. 1d.**

Cell counting assay and imaging methods

We placed eight 150 μL samples from each of the six cell concentrations into 48 individual wells of a 96-well plate (MatTek, P96G-0-5-F). The cells settled on the bottoms of the wells in a single layer. We imaged the 96-well plate from below, with four microscopes held in an inverted configuration. Four microscopes were mounted in a holder, which was also used for the zebrafish assay, and aligned with the well plate such that the field of view of each microscope was positioned over the center of its corresponding well. Independent focusing and control for each microscope permitted individual adjustments as needed. We acquired 3-5 non-overlapping images from each well, taken in parallel in sets of four wells for the entire 48-well assay. We also took for each well a background image without cells in focus. An image-processing algorithm (see below) determined cell counts for each well and thus cell concentration estimates for each dilution.

Algorithms for image processing and cell counting

We wrote custom software in MATLAB to count cells within raw images and estimate cell concentrations (**Supplementary Fig. 1d**). To correct for any background fluorescence not emitted by the cells, for each raw image we performed a background subtraction using the image of the same well of the 96-well plate but with the cells out of focus. To correct for any non-uniformities in illumination, we equalized contrast distributions across the image by applying the MATLAB function `histeq()`. This broke the full image into local regions (64 × 64 pixels) and equalized contrast by transforming the pixel intensities within each region so that the resulting pixel intensity

histograms would be approximately uniform across the full image. We cropped the contrast-adjusted image to a central portion (400 × 400 pixels, corresponding to 460 μm × 460 μm in the specimen plane) that we used for further analysis.

We converted the cropped image to binary format by using a sliding-window approach to finding regional maxima in intensity values. First, we found the maximum pixel value within a 7 × 7 pixel window. If this maximum value was greater than a threshold level, we converted all pixels in the window with intensities within 95% of the maximum to white. We made all other pixels within the window black. We determined the threshold level by Otsu's method, which selects a threshold value that minimizes intensity variations within the black and the white pixel classes based on the grayscale image histogram[42]. We slid the 7 × 7 window across the entire field of view, converting all pixels to binary format.

We then performed an initial segmentation of the binary images into contiguous objects of white pixels, in which each white pixel was adjacent to at least one other white pixel in the object along any of the 4 cardinal or 4 diagonal directions. We removed all such objects with area < 5 pixels from the initial segmentation. These objects were too small to be cells and were generally debris or noise artifacts arising from contrast equalization.

We made an initial tally of cells within the resulting image by counting all objects of area < 150 pixels. A majority of cells were usually correctly identified as single cells and counted at this step, but a few clusters of cells generally remained. We segmented these remaining clusters with areas > 150 pixels into single cells via further processing

and updated the cell count. To do this additional segmentation we used an iterative approach to morphological filtering.

In each iteration of morphological filtering, we successively applied erosion and dilation filters[43]. For erosion, we eroded a white pixel by marking it black if < 50% of all pixels in its neighborhood (window size = 7 × 7 pixels) were white. During dilation, we dilated a black pixel by marking it white if > 80% of all pixels in its neighborhood (window size = 7 × 7 pixels) were white. After these two steps, we updated the cell count to include all new objects of area < 150 pixels. In this way, we applied successive iterations of erosion and dilation to segment cell clusters into individual cells. We found empirically that 10 iterations sufficed to segment all cell clusters that remained after initial segmentation. We applied this cell counting method to each of the 3–5 images taken of each sample well. Together with the known well volume, the cell counts determined the estimates of cell concentration. To validate the accuracy of the counting algorithm, we took randomly chosen fields-of-view from wells with varying cell concentrations and compared manual scoring of cells with the values obtained from the automated algorithm. The two counts typically differed by < 5%.

Tuberculosis imaging

We prepared slides from mycobacterial cultures and labeled them with auramine-O, a fluorescent stain that binds mycolic acids in cell walls of Mycobacterium tuberculosis. We imaged the specimens through a cover slip using an integrated microscope.

Imaging of CA1 hippocampus

Viral vector for expression of GCaMP3

The plasmid containing the GCaMP3 sequence[34] was a gift from Dr. Loren Looger of the

HHMI Janelia Farm Research Campus. GCaMP3 was cloned into an AAV backbone carrying the CaMKIIα promoter[44]. The recombinant AAV vectors were serotyped with AAV5 coat proteins and packaged by the Vector Core at the University of North Carolina. Titers were ~$2 \cdot 10^{12}$ particles/mL.

Animals and hippocampal surgery

Stanford APLAC approved all animal procedures. We used male C57/BL6 mice, aged 8–12 weeks. Mice underwent two surgical procedures under isoflurane (1.5% – 2%). In the first surgery, mice received stereotaxic injections of 250 nL viral vector (AAV2/5-CaMKIIα-GCaMP3) into hippocampal area CA1 (anteroposterior, –1.9 mm relative to Bregma, 1.4 mm mediolateral, –1.65 mm dorsoventral). We injected the virus using a 10 μL syringe and a 33-gauge metal needle (World Precision Instruments). In the second surgery, one week after viral transduction, we implanted a glass optical guide tube just dorsal to area CA1 as previously described[33]. This guide tube was fixed to the cranium with dental acrylic and allowed repeated insertion of micro-optical probes to the same imaging site.

Image-guided installation of the microendoscope

Approximately 4 weeks after the second surgery, we performed an image-guided installation of the microendoscope into the optical guide tube while the mice were anesthetized with isoflurane. Two-photon imaging of CA1 for guiding the installation was performed through the microendoscope itself, following our lab's standard, published procedures[33,39,45]. In brief, we inserted a microendoscope that was a singlet gradient refractive index (GRIN) relay lens (GRINtech GmbH, GT-IFRL-100, 0.44 pitch length, 0.47 NA) into the guide tube, to relay light between the specimen plane in CA1

and the microscope objective located outside the animal. After verifying uniform expression levels of GCaMP3 and a healthy appearance of the hippocampal tissue, we permanently affixed the GRIN lens in the guide tube using UV-curing optical adhesive (Norland Products, NOA 81).

Imaging CA1 hippocampus in behaving mice

We positioned and installed the integrated microscope while the mice were anesthetized with isoflurane (1.5–2%). Using a translation stage we held the integrated microscope above the GRIN relay lens that had been affixed in the guide tube. We lowered the microscope towards the GRIN lens until we saw a fluorescence image of the virally labeled brain tissue using 0.05–0.2 mW of illumination power from the microscope's LED. After locating a suitable imaging site and focal depth, we turned off the LED and attached the microscope's base plate to the cranium using Cerebond™ adhesive (myNeuroLab.com, 39465030) and dental acrylic (Henry Schein, 5478203EZ). We began imaging when the mouse recovered from anesthesia.

References

42. Otsu, N. A threshold selection method from gray-level histrograms. *IEEE Trans. Sys. Man. Cyber.* **9**, 62-66 (1979).
43. Gonzales, R. & Woods, R. *Digital Image Processing*. (Prentice Hall, 2008).
44. Gradinaru, V. *et al.* Targeting and readout strategies for fast optical neural control in vitro and in vivo. *J Neurosci* **27**, 14231-14238 (2007).
45. Barretto, R. P. J. & Schnitzer, M. J. in *Imaging: A Laboratory Manual* (ed R. Yuste) Ch. 50, (Cold Spring Harbor Laboratory press, 2011).